13-17 January 2014, National Harbor, Maryland
16th AIAA Non-Deterministic Approaches Conference

Uncertainty analysis of corrugated skin with random elastic parameters and surface topology

Abhishek Kundu *
Swansea University, Swansea, United Kingdom
F. A. DiazDelaO †
University of Liverpool, Liverpool, United Kingdom
Michael I. Friswell ‡ and Sondipon Adhikari §
Swansea University, Swansea, United Kingdom

Uncertainty analysis of corrugated skins has been performed for random perturbations in geometric and elastic parameters of a chosen baseline model. The corrugated skins are particularly suitable for morphing applications in aerospace structures and their sensitivity to the various input uncertainties is a major concern in their design. The various sources of uncertainty include random perturbations of the geometrical parameters of the corrugation units, surface roughness and parametric uncertainty of the elastic parameters. These uncertainties are described here within the probabilistic framework and have been incorporated into the discretized stochastic finite element model used for their analysis. The propagation of these uncertainties to the dynamic response of the structure is a computationally intensive exercise especially for high dimensional stochastic models. Such high dimensional models have been resolved with statistical methods such as Gaussian Process Emulation and polynomial interpolation based sparse grid collocation techniques. The brute force Monte Carlo simulation technique results have been used as benchmark solutions. A global sensitivity analysis has been performed to identify the key uncertainty sources which affect the system response and the equivalent models using Sobol's importance measure.

I. Introduction

SIGNIFICANT research endeavor has been directed at designing light weight, highly compliant structures to implement the concept of 'shape morphing' in morphing aircraft technology. The requirement of almost contradictory elastic behavior of the materials, such as high flexibility along with sufficient rigidity has led to investigation into novel design of components with innovative microstructural arrangements to provide passive solutions (such as honeycomb composites, corrugated skins) along with smart technologies such as shape memory alloy actuators, embedded piezoelectric patches or shape memory polymers. The geometric and parametric modelization of small length scale structural features and variations are essential for simulation studies and can potentially have significant influence on their performance efficiency. Also, the equivalent low fidelity models, which are created for these structural components especially when representing them at higher length scales, needs to be able to provide an estimate of the sensitivity of the performance indicators to the various input parameters.

Studies of various composite structures offering enhanced mechanical and aerodynamic load bearing capacity have been reported in the literature. The concept of variable stiffness laminates is essential in this respect.[1] They utilize various local fibre orientation angles,[2] or curvilinear fiber path in laminates[3,4] to extend the range of elastic behavior of conventional materials. A review of the optimization algorithms for the variable stiffness composites is given by Ghiasi *et al*.[5] The state of the art research into morphing technology with various multifunctional composite materials having novel microstructural characteristics has been studied actively for their wide range of mechanical

*PhD Student, Aerospace Engineering, College of Engineering, Swansea University, Singleton Park, Swansea SA2 8PP, UK, Email: a.kundu.577613@swansea.ac.uk; AIAA Student Member.
†Lecturer, Centre for Engineering Dynamics, College of Engineering, University of Liverpool, Email: f.a.diazdelao@liverpool.ac.uk.
‡Professor of Aerospace Structures, College of Engineering, Swansea University, Email: m.i.friswell@swansea.ac.uk.
§Professor of Aerospace Engineering, College of Engineering, Swansea University, Email: S.Adhikari@swansea.ac.uk; AIAA Senior Member.

behavior. These belong to the class of passive methods which aim to define the material properties, their geometry, topology a-priori as per the predetermined design requirements. The objective functions in the optimization of these structural components incorporates compliance, rigidity, weight, damping and dynamic aeroelasticity among other factors. The auxetic honeycombs with varying cell geometry and infill stiffness has been studied[6] which produce high Young's modulus and damping loss. Morphing aircraft skins for passive applications using an elastomer-fibre-composite surface supported with flexible honeycomb structures have shown a high increase in surface area while maintaining aerodynamic load bearing capacity.[7] The various passive/active morphing technologies employed in aerospace applications has been reviewed.[8,9] Additionally, cellular honeycomb core composites have been used to design compliant members which have been reported to produce enhanced elastic behavior.[10]

In the domain of smart materials, the use of shape memory materials[11] to produce adaptive structures for morphing applications has also received significant attention[12–15] and have been studied in context of various aerospace implementations.[16–18] These composites offer the advantage of a light-weight actuation system with efficient aerodynamic load bearing capability. Smart materials with active actuators embedded in them have been widely applied to noise[19,20] and vibration control[21,22] in aerospace applications. Piezoelectric actuators has been used for morphing wing flight control,[23] in composite laminates,[24,25] with carbon fibre/epoxy composites with bonded piezoelectric actuators[26] in order to meet a wide range of performance demands under operating conditions. A review of the active solutions used in morphing structures is given by Barbarino *et al*.[27]

The current research focuses on the use of a corrugated skin as a passive compliant member with sufficient load bearing capacity as a potential shape morphing solution. A review of the morphing skins has been provided by Thill *et al* .[28] which includes corrugated structures as low modulus membranes, hence as possible candidates for morphing skins. Numerical and experimental studies with corrugated skins[29–31] and the deformation characteristics of the morphing wings with corrugated composites and skins have been studied in the literature.[32,33] Corrugated carbon fibre composites have been used as candidate materials for morphing wings.[34] However, due to the intricate design of the corrugated skins, the parametric and geometrical properties of the skins required in the mathematical models can not be known for certain. Often these uncertainties are irreducible due to the cost associated with their precise measurement. The present work aims to quantify these uncertainties with a probabilistic description and propagate these uncertainties to the dynamic system response of the corrugated skins. Thus, the countable set of random variables used to model the input uncertainty would form the stochastic input space of the mathematical model. Propagating this input randomness of the physical system to the response quantities (such as displacement, pressure, velocity) can be tackled with various uncertainty propagation techniques.

To begin with, it is assumed that there is a baseline model of the corrugated skin which is deterministic in nature. Within this model, a probabilistic description is incorporated into the various elastic (such as the bending stiffness, volume density) and the definitions of the geometric parameters (such as the height, width, angles of corrugation, surface topology). The description is typically provided with a set of random variables which introduce random perturbations into the geometry and elastic properties of the skin. Various uncertainty propagation techniques for a wide variety of stochastic structural dynamic systems exist in the literature which range from non-intrusive statistical simulation methods (such as the crude Monte Carlo simulation (MCS) and its variants[35,36]) to non-statistical analytical methods which provide explicit functional relationships between the independent random variables used to model the problem (such as the perturbation methods,[37] the Neumann expansion method[38] and the Galerkin-based finite order chaos expansion methods[39]). Alternatively, there are sparse-grid stochastic collocation methods which rely on constructing the random solution using polynomial interpolation functions with a set of random responses evaluated at the zeros of these multidimensional stochastic interpolation functions.[40,41] This requires resolution of the random system response at the sparse grid collocation points in a Monte Carlo sense and hence is non-intrusive and trivially parallelizable. For high-dimensional stochastic problems, adaptive sparse-grid collocation techniques have been proposed which aims to represent the problem with few lower order terms.[42,43] The computational evidence indicates the effectiveness of the sparse grid stochastic collocation method compared to full tensor and Monte Carlo approaches.

We have compared the performance of the collocation technique to a metamodeling strategy, known as Gaussian process emulation.[44] It is based on the analysis and design of computer experiments[45,46] and on the concepts of Bayesian statistics. The non-expensive approximation to the output is made after evaluating a small number of points in the input space, hence reducing the required computer processing time. After conditioning on these training runs and updating a prior distribution, the mean of the resulting posterior distribution approximates the output of the simulator at any untried input, whereas it reproduces the known output at each design point. Gaussian process emulation has been implemented in various scientific fields with encouraging results, such as structural dynamics,[47] multi-scale analysis,[48] stochastic finite elements,[49] and domain decomposition[50] among many others.

Once the input geometric and/or the (elastic) parametric uncertainty has been propagated to the system response,

it would be essential to have a quantitative measure of the sensitivity of the solution to the various input uncertainty. This helps to identify the parameters which are most sensitive to the response statistics. This is accomplished with a sensitivity analysis which is carried out using the concept of Sobol indices[51] which gives a quantitative estimate of the sensitivity of the solution to each source of uncertainty for a large input stochastic dimension. Thus it is possible to make an informed decision about which uncertainties can be ignored safely and the threshold values of the input variability for an uncertainty to become significant.

II. Stochastic dynamical system with uncertain elastic and geometrical parameters

II.A. Description of stochasticity in a structural dynamic system

Consider a damped corrugated skin whose baseline model is given in figure 1. Such corrugated skins are prone to geometric uncertainties (due to manufacturing) and material uncertainties, such as a random bending stiffness. A deterministic model of this composite corrugated skin has been studied previously.[52] Figure 1(a) shows a sketch of

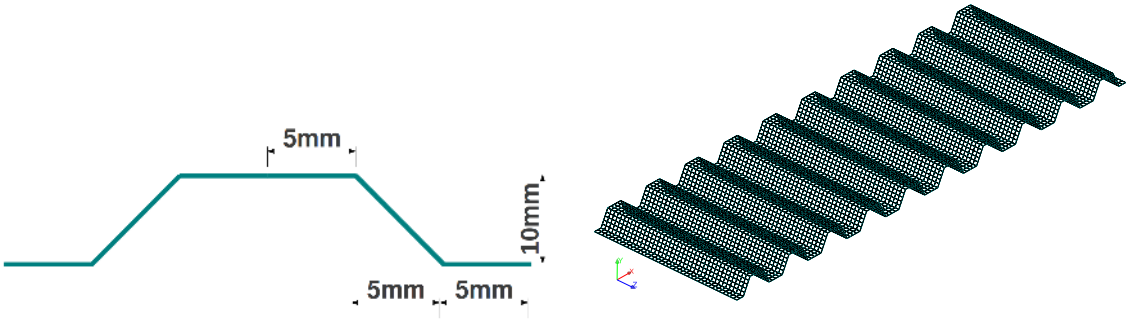

(a) Sketch of one corrugated unit (b) Meshed corrugated skin

Figure 1. Model of the corrugated skin employed in the analysis. (a) Unit cell; (b) Finite element model of the corrugated skin. The dimensions are: 300 mm in length, 75 mm in width, and 10 mm in height.

the side view of a unit cell with the corresponding geometry. Figure 1(b) shows the meshed geometry of the corrugated skin that has been employed in the analysis. This highly compliant skin is particularly important in morphing applications as discussed in section I.

A random field $a(\mathbf{r},\theta) : \mathcal{D} \times \Theta$ over a spatial domain $\mathcal{D} \in \mathbb{R}^d$, may be expressed in a series expandable form following a spectral decomposition of the associated covariance kernel with the random field as

$$\int_{\mathcal{D}} C_a(\mathbf{r}_1,\mathbf{r}_2)\varphi_j(\mathbf{r}_1)\mathrm{d}\mathbf{r}_1 = \nu_j\varphi_j(\mathbf{r}_2), \quad \forall\ j = 1,2,\cdots \tag{1}$$

The above is a homogeneous Fredholm integral equation of the second kind. If $\mathcal{C}_a\varphi$ is defined as $(\mathcal{C}_a\varphi)(\mathbf{r}_2) = \int_{\mathcal{D}} C_a(\mathbf{r}_1,\mathbf{r}_2)\varphi(\mathbf{r}_1)d\mathbf{r}_1, \quad \mathbf{r}_1,\mathbf{r}_2 \in \mathbb{R}^d$, it can be verified that $\mathcal{C}_a : L^2(\mathbb{R}^d) \to L^2(\mathbb{R}^d)$ is a linear operator on a vector space. Hence Eq. (1) can be expressed as $\mathcal{C}_a\varphi = \nu\varphi$. A non-trivial solution to the above homogeneous equation exists only for those values of ν which make $(I-\nu\mathcal{C}_a)$ singular, where I is the identity operator. The covariance functions C_a are usually bounded and symmetric, hence the associated linear operator $\mathcal{C}_a$ is compact and self-adjoint. The solution of the eigenvalue problem in (1) yields ordered real eigenvalues $\nu = \{\nu_i : \nu_i \geq \nu_{i+1}\ \forall i$ and $\|C_a\|^2_{L^2\left(\mathbb{R}^d\times\mathbb{R}^d\right)} = \sum_i \nu_i^2\}$ and mutually orthogonal eigenfunctions $\varphi(\mathbf{r}_1)$ in $L^2(\mathbb{R}^d)$. Thus, from Mercer's theorem we can write

$$C_{a_M}(\mathbf{r}_1,\mathbf{r}_2) = \sum_{i=1}^{M} \nu_i\varphi(\mathbf{r}_1)\varphi(\mathbf{r}_2) \tag{2}$$

where C_{a_M} converges uniformly to C_a as $M \to \infty$.

The covariance function might not always be a continuous function of the spatial domain, and it is possible to have a correlation between the various parameters which can only have discrete indices. For example, the width or height of the corrugation between different corrugation units or the angles of corrugation ϕ_i within one corrugation unit and across various units. The description of these uncertainties requires a discrete covariance function. For these cases, the linear operator $\mathcal{C}_a$ has finite dimensional eigenvectors as its solution of Eq. (1). Thus the random field can be

represented with a denumerable set of eigenvalues and eigenvectors of the covariance kernel using the Karhunen-Loève (KL) expansion as

$$a(\mathbf{r},\theta) = a_0(\mathbf{r}) + \sum_{i=1}^{M} \sqrt{\nu_i}\widetilde{\xi}_i(\theta)\varphi_i(\mathbf{r}), \tag{3}$$

where $a_0(\mathbf{r}) = \mathrm{E}\left[a(\mathbf{r},\theta)\right]$ is the mean, and $\widetilde{\xi}_i(\theta)$ are the mutually independent random variables with zero mean ($\mathrm{E}\left[\widetilde{\xi}_i\right] = 0$) and unit variance ($\mathrm{E}\left[\widetilde{\xi}_i^{\,2}\right] = 1$) for $i = 1,\ldots,M$. The above expansion is valid for Gaussian random fields. General non-Gaussian random fields are expressed in a mean-square convergent series using the Wiener-Askey chaos expansion scheme,[53,54] where the basis functions are constructed with a denumerable set (M) of independent random variables $\boldsymbol{\xi} = [\xi_1,\xi_2,\ldots,\xi_M]^\intercal \in \Theta^{(M)}$ where $\Theta^{(M)} \subset \Theta$. These basis functions span the stochastic Hilbert space and hence the problem can be equivalently formulated on a finite dimensional probability space $\left(\Theta^{(M)},\mathcal{F}^{(M)},P^{(M)}\right)$ where $\Theta^{(M)} = \mathrm{Range}(\boldsymbol{\xi})$, $\mathcal{F}^{(M)}$ is the associated Borel σ-algebra and $P^{(M)}$ is a probability measure. The formulation presented in this paper is applicable to this kind of general decomposition of the random field.

II.B. Stochastic partial differential equation for the dynamical system

The corrugated skin presented in the previous section is taken to have uncertainties both in the material and geometric properties which have been described probabilistically. This requires the uncertainty to be expressed with a set of finite number of independent random variables. These random variables constitute the input stochastic space. We present here the analysis of the parametric and geometric uncertainties in separate discussions.

II.B.1. Parametric uncertainty

A randomly parametrized structural dynamic system is defined on the domain $\mathcal{D} \subset \mathbb{R}^d$ ($d \leq 3$), with piecewise Lipschitz boundary $\partial\mathcal{D}$, subject to an externally applied deterministic excitation f_0. The equilibrium condition gives the following stochastic partial differential equation (SPDE)

$$\rho\frac{\partial^2 u}{\partial t^2} + \mathfrak{L}_\eta\frac{\partial u}{\partial t} + \mathrm{div}(\sigma_a(u)) = f_0 \quad \text{ on } \mathcal{D},\ \ t \in \mathbb{R}^+ \tag{4}$$

with the associated Dirichlet boundary condition

$$u = 0 \quad \text{ on } \partial\mathcal{D}.$$

where $\sigma_a(u)$ is the stress related to the displacement field u, ρ is the mass density, and t is the time. $\mathfrak{L}_\eta$ denotes the damping operator, with η as the damping parameter, and can be used to represent different damping models such as strain rate dependent viscous damping or velocity dependent viscous damping. $(\Theta,\mathcal{F},P)$ is a probability space where $\theta \in \Theta$ is a sample point from the sampling space Θ, $\mathcal{F}$ is the associated Borel σ-algebra and P is a probability measure. The constitutive equations relating the stress field to the displacement u is given as

$$\sigma_a(u) = a(\mathbf{r},\theta) : \varepsilon(u)$$

where a is the Hooke's elasticity tensor and is a second order, stationary, square integrable random field such that $a : \mathbb{R}^d \times \Theta \to \mathbb{R}$. Here ':' denotes the standard tensor inner product of second order tensors. Depending on the physical problem, the random field $a(\mathbf{r},\theta)$ can be used to model different physical systems.

For the harmonic analysis of the system Eq. (4) is written in the frequency domain (using Fourier transformation) as

$$-\omega^2\rho\widetilde{u} + i\omega\left(\mathfrak{L}_\eta\widetilde{u}\right) + \mathrm{div}\left(\sigma_a(\widetilde{u})\right) = \widetilde{f}_0(\omega) \qquad \omega \in \Omega, \tag{5}$$

where Ω denotes the frequency space of the problem. Here $\widetilde{f}_0(\omega)$ and $\widetilde{u}(\omega)$ are the frequency dependent complex amplitudes of the harmonic input excitation and the system response respectively.

The FE treatment of the governing SPDE involves spatial discretization of the continuum $\mathcal{D} \in \mathbb{R}^d$ into domains with polygonal boundaries $\mathcal{D}^h$ where h is the mesh space parameter. From the Doob-Dynkin lemma for the parametrized equation in Eq. (4), where the input randomness is expressed in terms of a finite dimensional vector $\boldsymbol{\xi}(\theta)$ (as in (3)), the solution can be expressed entirely in terms of the same random variables. Thus the solution of the discretized FE system is sought in the Hilbert space $\mathcal{H}(\mathcal{D}^h \times \Theta)$. This space can be expressed in a separable form with

the Hilbert spaces $\mathcal{H}_1$ and $\mathcal{H}_2$ such that $\mathcal{H} \simeq \mathcal{H}_1 \otimes \mathcal{H}_2$. The well established techniques of variational formulation of the displacement-based deterministic finite-element method then gives us the following form of the stochastic system matrices[55] using the stochastic discretization technique illustrated in section II.A. The system matrices inherit the randomness of the input stochastic parameters and hence the stochastic linear system for structural dynamics takes the form

$$\begin{aligned} \left[-\omega^2\mathbf{M}(\theta) + j\omega\mathbf{C}(\theta) + \mathbf{K}(\theta)\right]\widetilde{\mathbf{u}}(\omega,\theta) &= \widetilde{\mathbf{f}}_0(\omega) \\ \text{or,} \quad \left(\mathbf{A}_0(\omega) + \sum_{i=1}^{M}\xi_i(\theta)\mathbf{A}_i(\omega)\right)\widetilde{\mathbf{u}}(\omega,\theta) &= \widetilde{\mathbf{f}}_0(\omega) \end{aligned} \tag{6}$$

where $\mathbf{M}(\theta)$, $\mathbf{C}(\theta)$ and $\mathbf{K}(\theta)$ are the random mass, damping and stiffness matrices respectively, which have been combined to obtain the complex frequency dependent coefficient matrices $\mathbf{A}_i(\omega),\ i = 0, 1, \ldots, M$. Also,

$$\mathbf{M}(\theta) = \mathbf{M}_0 + \sum_{i=1}^{p_1}\mu_i(\theta)\mathbf{M}_i \in \mathbb{R}^{n\times n} \quad \text{and} \quad \mathbf{K}(\theta) = \mathbf{K}_0 + \sum_{i=1}^{p_2}\nu_i(\theta)\mathbf{K}_i \in \mathbb{R}^{n\times n} \tag{7}$$

Here ($\mathbf{M}_0$ and $\mathbf{K}_0$) are the deterministic mass and stiffness matrices while ($\mathbf{M}_i$ and $\mathbf{K}_i$) are the corresponding perturbation components obtained from discretizing the mass and stiffness parameters with finite number of random variables ($\mu_i(\theta)$ and $\nu_i(\theta)$). The total number of random variables utilized to represent the stochastic system matrices is $M = p_1 + p_2$. We have chosen the proportional damping model in the present work where the damping parameter is expressed as a linear combination of the mass matrix and the system stiffness matrix.

For the proportional damping model considered here $\mathbf{C}(\theta) = \zeta_1\mathbf{M}(\theta) + \zeta_2\mathbf{K}(\theta)$, where ζ_1 and ζ_2 are deterministic scalars. Hence the expressions for the coefficient matrices are given by

$$\mathbf{A}_0(\omega) = \left[-\omega^2 + j\omega\zeta_1\right]\mathbf{M}_0 + \left[j\omega\zeta_2 + 1\right]\mathbf{K}_0 \tag{8}$$

$$\begin{aligned} \text{and,} \quad \mathbf{A}_i(\omega) &= \left[-\omega^2 + j\omega\zeta_1\right]\mathbf{M}_i \quad \text{for} \quad i = 1, 2, \ldots, p_1 \\ \mathbf{A}_k(\omega) &= \left[j\omega\zeta_2 + 1\right]\mathbf{K}_k \quad \text{for} \quad k = p_1+1, p_1+2, \ldots, p_1+p_2 \end{aligned} \tag{9}$$

The solution methodologies of the system given in Eq. (6) is presented in the following section.

III. Methodology and Results

The problem of structural vibration of the corrugated skin presented in figure 1 with random elastic and geometrical parameters has been considered here. As discussed earlier corrugated laminates offer a plausible solution for morphing aircraft skins due to their extremely anisotropic behaviour. The corrugation direction (chordwise direction) offers compliance and the spanwise direction (transverse to corrugation) makes the structure much stiffer. Corrugated skins are prone to geometric uncertainties (due to manufacturing) or material uncertainties, such as a random bending stiffness. We analyze such a composite corrugated skin[52] whose Young's modulus is taken as 16 GPa and its Poisson's ratio as 0.225.

Here we take the elastic parameters (such as the bending stiffness and the axial stiffness of the plate) to be modeled as random quantities. We model these parameters as the stationary Gaussian random field

$$\alpha(\mathbf{r}, \xi(\theta)) = \alpha_0(1 + \epsilon(\mathbf{r}, \xi(\theta)) \tag{10}$$

where α is the random parameter of the corrugated skin, $\mathbf{r}$ is the length along the physical dimensions of the corrugated skin and $\epsilon(\mathbf{r}, \xi(\theta))$ is a zero mean stationary Gaussian random field. The autocorrelation function of this random field has been assumed to be exponential. Thus if $\mathbf{r}_1 \neq \mathbf{r}_2$ then

$$C_\epsilon(\mathbf{r}_1, \mathbf{r}_2) = \sigma_\epsilon \exp\left\{-(|\mathbf{r}_1 - \mathbf{r}_2|)/\mu_\mathbf{r}\right\} \tag{11}$$

where $\mu_\mathbf{r}$ is the correlation length defined along the physical dimensions of the skin and σ_ϵ is the standard deviation associated with the random elastic parameters.

Figure 2 shows a few chosen eigenvectors associated with the KL expansion of the covariance kernel. Note that the random elastic parameters and the KL eigen modes are scalar quantities over the spatial domain. In order to facilitate better graphical representation of these quantities, they have been plotted as sidewise displacements (y-direction) of

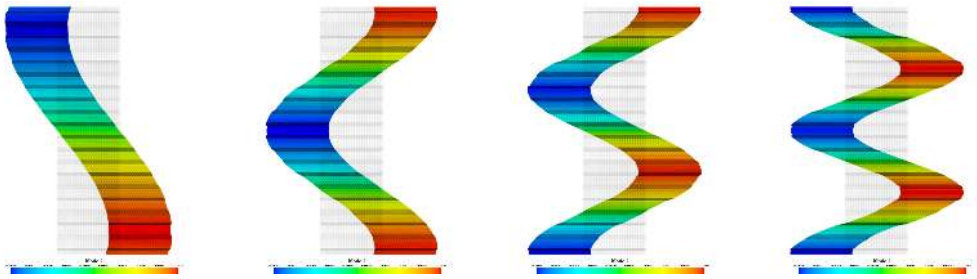

(a) 2^{nd} KL eigenvector (b) 3^{rd} KL eigenvector (c) 4^{th} KL eigenvector (d) 5^{th} KL eigenvector

Figure 2. Four different KL modes of the random field with an exponential covariance function for the random field. The eigenfunctions have been plotted as the sideways displacements of the skin to graphically highlight their nature.

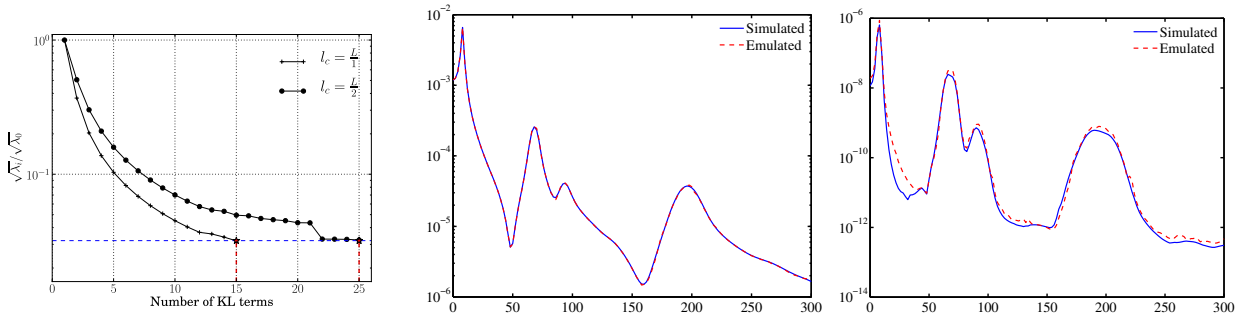

(a) The eigenvalue spectrum of the Covariance kernel (b) Mean FRF (c) SD of FRF

Figure 3. (a) The decay of the eigenvalue spectrum of the exponential covariance kernel of the corrugated plate for different correlation lengths defined as the L2 norm. Emulation and simulation of the mean frequency response (b) and standard deviation of the frequency response (c). The simulation was performed for every frequency level in the input domain, based on 10,000 samples. Only 250 samples were necessary to emulate the statistics of the frequency response at a comparable accuracy.

the skin. The higher modes are more complicated in shape which is similar to the behaviour of higher structural vibrational modes. However, it must be noted that these KL modes are not the same as the vibrational modes of the structural finite element system.

In order to decide the number of terms in the KL expansion, the eigenspectrum associated with the exponential covariance function is shown in figure 3(a) for two different correlation lengths $L/1$ and $L/2$ where L is the dimension of the physical domain of the problem. It is seen that the eigenvalues decay more rapidly for the larger correlation lengths indicating that fewer KL modes can capture most of the variability of the exponential kernel. For the stochastic vibration response analysis for (elastic) parametric uncertainty, we have chosen the correlation length to be $L/2$ and hence approximated the random field with the most dominant 25 eigen modes of the expansion. This sets the dimension of the input stochastic space and 25 independent identically distributed (iid) random variables were used to represent the discretized random elastic parameters in the spatial domain. The standard deviation of the random field is assumed to be $\sigma_\epsilon = 0.1$. The analysis described above was repeated across the entire frequency range of 0-300Hz. For every frequency level ω, the Bayesian uncertainty analysis was performed and statistics of the FRF were obtained. This has been compared with the brute force MCS simulation. Figures 3(b) and 3(c) shows the emulated mean and standard deviation of the FRF respectively.

The Bayesian metamodel has been used to compute the system response from a set of sample stochastic solutions which constitute the training runs. The sample points for the training runs are generated using a space-filling strategy, such as a Latin hypercube. Each design point is drawn from the input distribution $\mathcal{F}(\boldsymbol{\xi})$, a multivariate standard normal random variable in the high-dimensional stochastic space. The design points are evaluated and the corresponding system response is reconstructed. The resulting training runs for each frequency level are of the form $\left(\boldsymbol{\xi}^{(i)}, \widetilde{\mathbf{u}}(\boldsymbol{\xi}^{(i)}, \omega)\right)$ for $i = 1, \ldots, 250$ which are used to obtain the mean, variance and the posterior distribution of the stochastic system response. Figure 4 exemplifies the accuracy of such an approximation for some fixed frequency levels which compare the cumulative distribution functions (cdfs) of the simulated and emulated outputs. 95% credible intervals for the emulated cdfs are also displayed. The advantages of Bayesian emulation become apparent: while every MCS run is

independent, Bayesian emulation takes advantage of the information that each design point contains about the nearest design points.

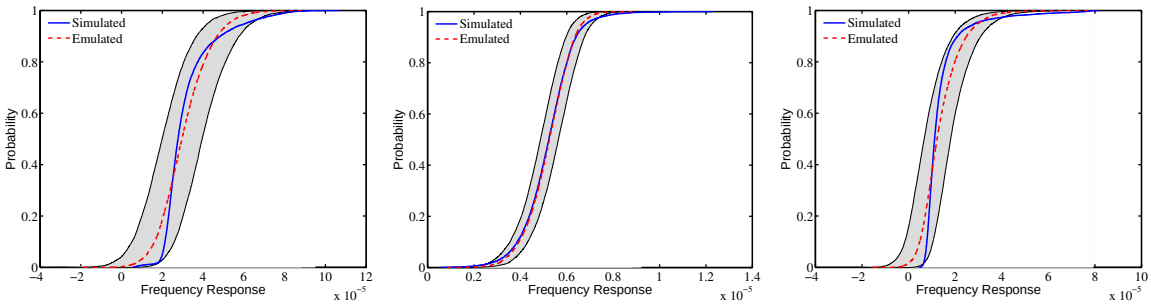

(a) Empirical cdf at 98Hz (b) Empirical cdf at 138Hz (c) Empirical cdf at 214Hz

Figure 4. Comparison between emulated and simulated cdfs for different frequency levels. 95% credible intervals (shaded areas) are shown for the cdfs.

Once the posterior distribution has been computed, any statistical summary of the output distribution can be estimated by drawing a large sample from the input distribution $\mathcal{F}(\boldsymbol{\xi})$ and using the samples generated from the posterior distribution to estimate the summary. The process is illustrated in figure 5, where samples of increasing size are drawn from the posterior distribution in order to estimate the mean of the output distribution. The prediction is contrasted with 10,000 Monte Carlo samples. It can be seen how the variance of the sample mean estimated via Bayesian emulation is reduced. Note however that this variance will always be greater than the Monte Carlo variance, since the emulator is built upon a finite number of training runs, and there will always be a lack of information due to this smaller set of simulator evaluations. The choice of the number of random functions is guided by the accuracy requirement

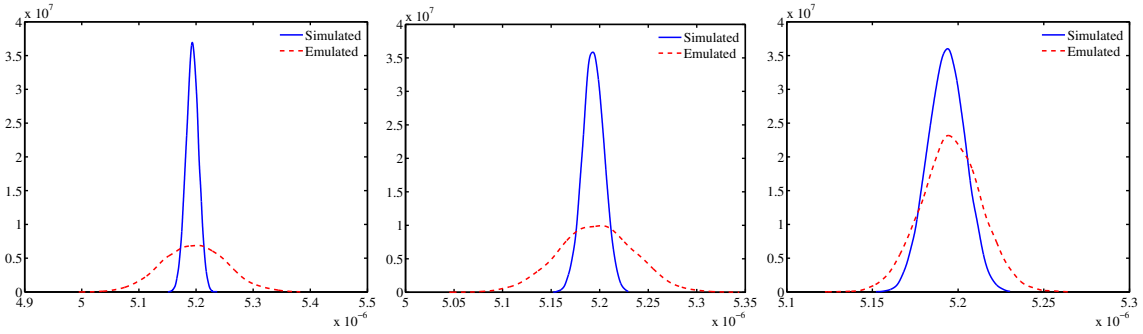

(a) $N = 1000$ (b) $N = 5000$ (c) $N = 10000$

Figure 5. Simulated vs emulated mean of the sample distribution. As the number of generated random functions necessary to approximate the solution increases, the variance of the sample mean decreases. This means that uncertainty about the sample mean results from the lack of information due to the computational cost of the original simulator.

and consideration for computational cost. Also, the error in the emulation can be quantified based on the emulation methodology and hence there is a measure of the accuracy of the pdfs obtained in figure 5.

III..2. Geometric uncertainty

Each corrugation unit of the skin given in figure 1 is defined by its width, height and the angle of corrugation. However, it is impossible to have an exact replication of the prescribed geometrical parameters given in the mathematical model. The aim here is to account for this uncertainty in the corrugation geometry and investigate its effect on the response and the equivalent stiffness of the corrugated skin. Additionally there might be random surface roughness present in the corrugated skin which can be quantified with the correlation of the position coordinates as a function of the distance between two points. Figure 6 is a graphical representation of the arbitrary perturbation of the height, angle and width of corrugation superimposed on a random surface topology of the baseline model. The randomness in the surface topology has been considered to be independent of the variations in the dimensions of the corrugation.

For any scalar field (such as the elastic parameters, or the position coordinates) and irrespective of the correlation length, the eigenfunctions obtained for the KL expansion of the covariance kernel have the exact shape as those given in figure 2.

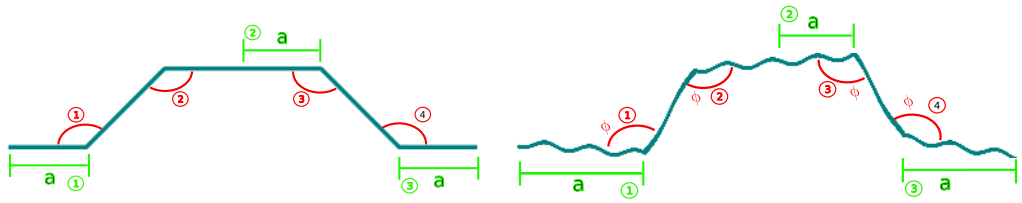

(a) Baseline corrugated unit (b) Perturbed corrugated unit

Figure 6. Perturbation of a corrugated unit for arbitrary randomness of the various geometrical parameters and random surface topology.

For the above random geometry, obtaining the system matrices with polynomials of the random variables used to model the perturbation of the positional coordinates, is mathematically quite cumbersome. Hence the spectral Galerkin methods, where the solution is expressed with a set of orthogonal polynomials of the input random variables, is not the obvious first choice. We have solved the random surface topology corrugated skin problem with stochastic collocation techniques where the system has been solved at a set of quadrature points in the input stochastic space. Hence the solution can be reconstructed in the high dimensional (M) stochastic space with polynomial basis functions of the random variables as

$$\mathcal{U}^{i_1} \otimes \ldots \otimes \mathcal{U}^{i_M} = \sum_{j_1=1}^{m_{i_1}} \ldots \sum_{j_M=1}^{m_{i_M}} f(x_{j_1=1}^{i_1}, \ldots, x_{j_M=1}^{i_M}) \cdot \left(a_{j_1}^{i_1} \otimes \ldots \otimes a_{j_M}^{i_M}\right) \tag{12}$$

$$\text{where} \quad \mathcal{U}^{i_k}(f) = \sum_{j=1}^{n_i} f(x_j^{i_k}) \cdot a_j^{i_k}$$

is the approximation of the random field along each stochastic dimension. The above tensor product formula requires evaluation of the stochastic objective function at $(m_{i_1} \ldots m_{i_M})$ grid points. For very high dimensional problems, i.e. large M, the above method becomes computationally intensive and a sparse grid technique is implemented using Smolyak's algorithm as[56]

$$\mathcal{A}(q, M) = \sum_{q-M+1 \le |\mathbf{i}| \le q} (-1)^{q-|\mathbf{i}|} \cdot \binom{M-1}{q-|\mathbf{i}|} \cdot \mathcal{U}^{i_1} \otimes \ldots \otimes \mathcal{U}^{i_M} \tag{13}$$

where $\mathcal{A}(q, M)$ are linear combinations of product formulas given in Eq. (12), $q \geq M$ and $\mathbf{i} = (i_1, \ldots, i_M)$ with $|\mathbf{i}| = i_1 + \ldots + i_M$ which requires fewer realizations of the stochastic response in order to obtain the complete response statistics. Hence to compute $\mathcal{A}(q, M)$ the response has to be evaluated at the sparse grid points

$$\mathcal{X}(q, M) = \bigcup_{q-M+1 \le |\mathbf{i}| \le q} \left(X^{i_1} \times \ldots \times X^{i_M}\right) \tag{14}$$

with $X^{i_k} = \left\{x_1^{i_k}, \ldots, x_{m_i}^{i_k}\right\}$ denoting the set of points used by $\mathcal{U}^{i_k}$. Here we have used the Smolyak formulas that are based on polynomial interpolation at the extrema of the Chebyshev polynomials. This gives a nested set of nodes which can be used to approximate the stochastic quantity.

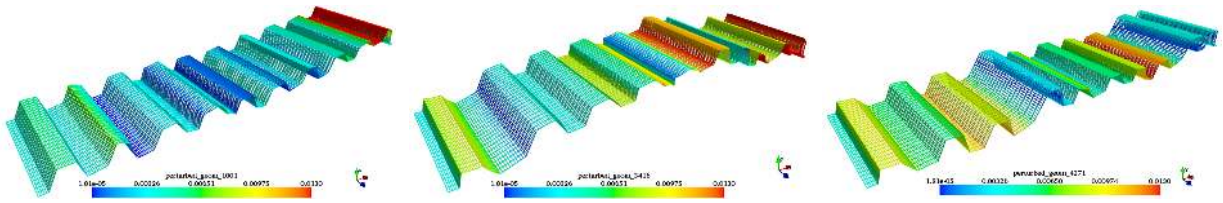

(a) Random Sample 1 (b) Random Sample 2 (c) Random Sample 3

Figure 7. Random realizations of the corrugated skin with stochastic geometrical properties. Here the geometry of the corrugation such as the length, width and height has been considered as random and has been modeled with 25 iid Gaussian random variables.

Hence for each point $x \in \mathcal{X}(q, M)$, the finite element system to be solved is given by the random realizations of the position coordinates obtained using the KL eigen modes. We present in figure 7 some realizations of the random geometry of the corrugated skin where the geometrical parameters of the corrugation (such as the width, angle, height of

corrugation) have been perturbed. Figure 8 gives the corrugated skin which has random dimension of the corrugations obtained for a model of random surface roughness along the length-wise direction (x-axis). Here the correlation length has been taken as a 100^{th} of the length of the skin. Careful observation reveals that the major difference between the perturbations introduced in figures 7 and 8 is that in the former case the perturbation is introduced in the corrugation geometry while the latter case constitutes a model of surface roughness.

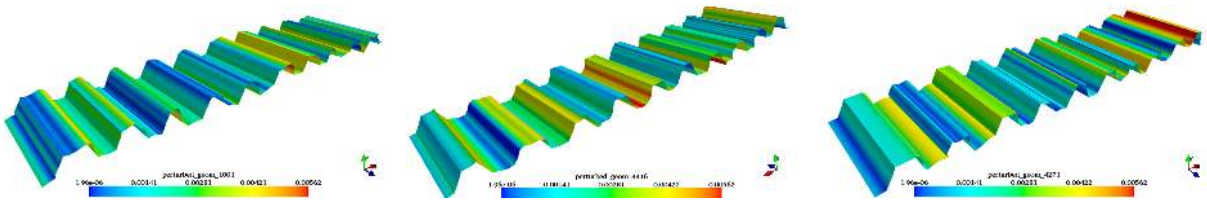

(a) Random Sample 1 (b) Random Sample 2 (c) Random Sample 3

Figure 8. Random realizations of the corrugated skin with stochastic geometrical properties for random surface topology. Here the surface roughness has been modeled with 100 random variables with a correlation length of one-hundredth of the length of the original skin.

We have obtained the solution of this system with the dimension-adaptive stochastic collocation method where the finite element solver has been employed to obtain the solution at a set of points in the stochastic space. The random geometry has been approximated with 25 iid random variables. When dealing with high-dimensions in the stochastic space, such as this, a full tensor grid solution of the stochastic problem becomes prohibitively expensive. Hence we have utilized dimension-adaptive sparse grids which adaptively refine the interpolant with respect to the dimensions that are most important. This is determined from the hierarchical surpluses calculated at a small sets of points.

It is known that the propagation of multiplicative input uncertainty to the system response leads to the stochastic solutions which can be expressed as polynomials of random variables. The accuracy of finite order polynomial interpolation of course depends on the smoothness of the function. Under the assumptions of moderately smooth response functions, we have used the Chebyshev-Gauss-Lobatto grid[56] to approximate the response. This is based on polynomial interpolation of the objective function in the stochastic space and hence produces good approximations of the solution. Additionally, this scheme has the benefit of nesting of nodes which has substantial computational advantage.

The dynamic response of the corrugated skin with geometric uncertainty is given in figure 9 with the sparse grid collocation scheme outlined above. The stochastic dimension is 25 and comprises of iid Gaussian random variables. The stochastic sparse grid for this problem with 25 dimensions, and with just 2 points along each direction would

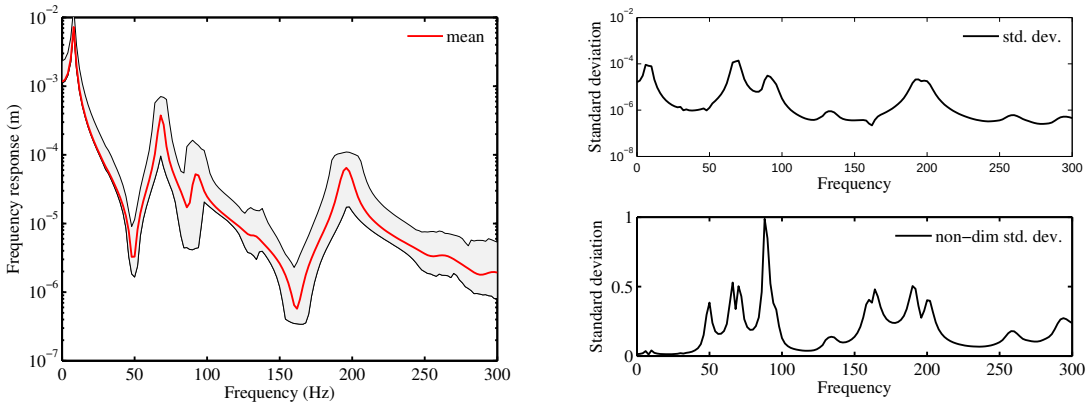

(a) Mean of the response (b) Standard deviation of the response

Figure 9. (a) Mean frequency response function in the ensemble of the various reponse functions obtained for each sample realization of the random geometrical configuration of the corrugated skin. The sample realizations frequency response functions have been obtaained with a dimensional-adaptive sparse grid collocation techique using Chebyshev interpolation functions. The random geometry has been approximated with 25 independent identically distributed random variables. (b) Standard deviation of the response and the corresponding non-dimensional standard deviation obtained by normalization with the mean response.

amount to a staggering 3.36×10^7 points in the stochastic space. In contrast, the proposed adaptive sparse grid method produces a solution of accuracy $\approx 10^{-4}$ with as few as $8,000$ sample points.

Figure 9 shows that the variability of the frequency response of the corrugated skin with random geometry is more pronounced at resonance frequencies beyond 50 Hz. The plot for the non-dimensionalized standard deviation

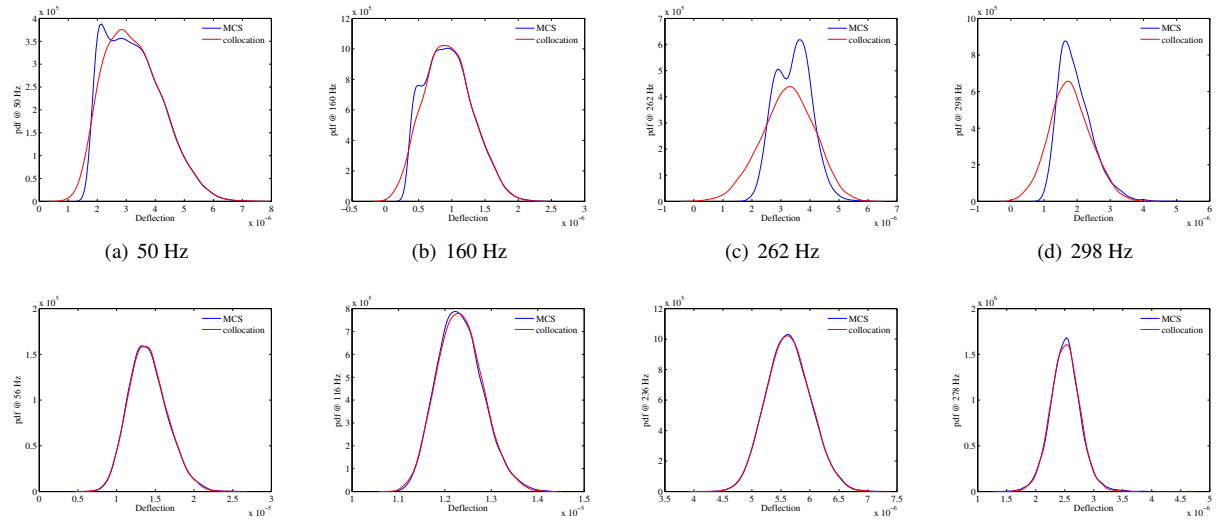

(a) 50 Hz (b) 160 Hz (c) 262 Hz (d) 298 Hz

(e) 56 Hz (f) 116 Hz (g) 236 Hz (h) 278 Hz

Figure 10. Probabilty density functions of the dynamic reponse of the corrugated skin at different (a) resonance and (b) non-resonance frequencies. The density functions have been constructed from the system response approximated with the dimension adaptive collocation technique and compared to the direct Monte Carlo simulation results.

of the frequency response shows that the fundamental mode at $\approx$ 10 Hz does not have a very large variability due to input random geometry. However, beyond 50 Hz, the resonance and anti-resonance modes generally have high values of standard deviation associated with them. Also, the general level of variability in the response increases at higher frequencies. This observation leads to the conclusion that the geometric variability in the form of surface roughness, as shown in figure 8, affects the more complicated higher vibration modes than the fundamental modes. This is understandable since the vibration energy is more localized at higher frequencies and hence is affected by the surface randomness present in the corrugated skin.

The probability density functions of the response at various frequencies (resonant and non-resonant) are shown in figure 10. The set of figures in the upper row, Figure 10(a)–10(d), correspond to the response at resonance frequencies while those in the lower row, figure 10(e)–10(h), give the same for non-resonant frequencies. It can be seen that a better approximation of the response is obtained with the collocation technique near the non-resonant frequencies. A higher number of grid points is necessary to obtain a better approximation of the response and to match the pdf obtained for the brute force Monte Carlo method. 25,000 samples have been used to obtain the MCS simulation results.

We now focus on the relative importance of the set of 25 random variables which model the random geometry by analyzing the sensitivity of the response to each of them. To begin with, the scatter plot of the dynamic response with respect to the second, fifth and the eleventh random variable is shown in Figure 11. The scatter plots are shown for two different frequencies 40 Hz and 152 Hz. The various sample responses were obtained by interpolating the stochastic system response with the above mentioned sparse grid collocation method. The clearly identifiable pattern from these plots indicates that the response is more sensitive to the second and fifth random variables compared to the eleventh. The ordering of the random variables is based on the decreasing eigenspectrum of the covariance function (as detailed in section II.A) describing the surface roughness of the corrugated skin.

A quantitative estimate of the sensitivity of the response to these various random variables is provided by the Sobol indices.[51] Considering that the random samples $\mathbf{x}$ are found in $\mathbf{x} \in \mathcal{X}$ where $\mathcal{X}$ is a rectangle of $\mathbb{R}^M$, the first order Sobol indices of the stochastic response $\widetilde{u} : \mathcal{X} \subset \mathbb{R}^M \rightarrow \mathbb{R}$ are defined as

$$\mathcal{S}_i(\widetilde{u}) = \frac{\mathrm{Var}\left[\mathrm{E}(\widetilde{u}(\mathbf{x})|\mathrm{x_i})\right]}{\mathrm{Var}\left[\widetilde{u}(\mathbf{x})\right]}\,, \qquad i = 1, \ldots, M \tag{15}$$

This quantity can be evaluated from a set of sample solutions using either Monte Carlo based approaches or other schemes usually employed in the uncertainty propagation for randomly parametrized systems such as the stochastic spectral Galerkin or the collocation scheme. Alternatively, Gaussian Process Emulation is also readily applicable to the above equation. First we assume a prior about $\widetilde{u}$ in the form of a Gaussian process characterized by a covariance function with a set of parameters. We use a set of training runs to obtain the mean, variance and the posterior disrtibution of the stochastic system and the Sobol indices are based on only a few evaluations.

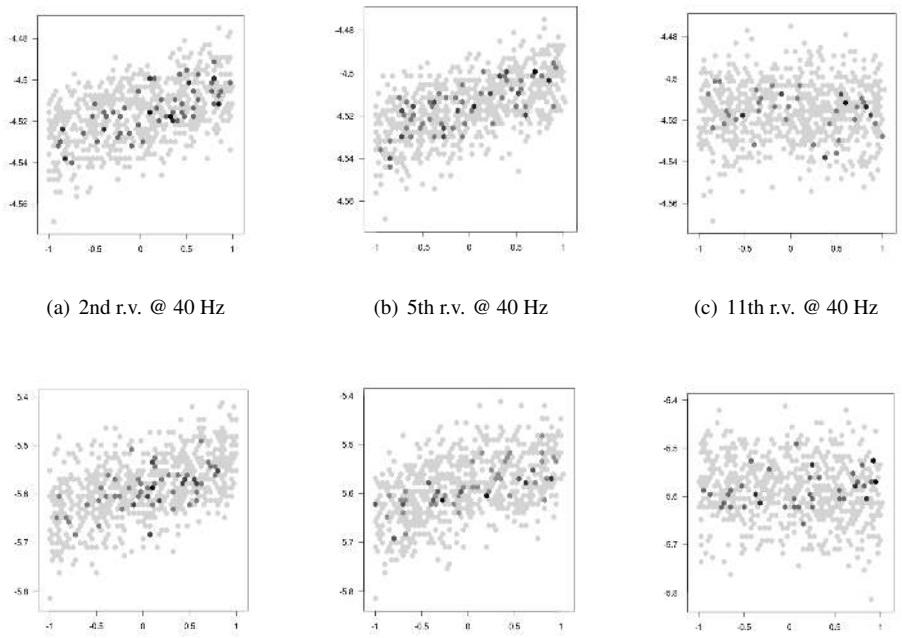

(a) 2nd r.v. @ 40 Hz (b) 5th r.v. @ 40 Hz (c) 11th r.v. @ 40 Hz

(d) 2nd r.v. @ 152 Hz (e) 5th r.v. @ 152 Hz (f) 11th r.v. @ 152 Hz

Figure 11. Scatter plots of the dynamic response of the corrugated skin with respect to the second, the fifth and the eleventh random variable modeling the random geometry at specific frequency steps. The y-axis gives the log value of the response where as the x-axis has the random variable values.

Table 1. First order Sobol indices and their credible intervals to obtain the sensitivity of the stochastic system response at 40 Hz to the various input random variables (the 2nd, 5th and 11th). The sample response has been approximated with the sparse grid collocation technique and the response has been interpolated at the stochastic sample points used for the estimation of the sensitivity indices.

Sensitivity Measure	RV Index 2	RV Index 5	RV Index 11
1st order Sobol indices	0.2712	0.5035	0.0016
Credible interval	0.0434	0.0711	0.0032

Utilizing the Sobol indices as the quantitative estimator, the second, fifth and the eleventh random variable at the frequency of 40 Hz is analyzed as given in table 1. The first order Sobol indices have been evaluated along with their respective credible intervals which indicate the accuracy of the evaluted indices. It is seen that a satisfactory accuracy is achieved for the more important (2nd and 5th) random variables. In case of geometric uncertainty, since the response of the stochastic system is a highly non-linear complex function of the input random variables, it is not known a-priori which random variables are most dominant. Especially for a high dimensional problem, where the geometric length scales associated with the input uncertainty (such as the correlation length) are quite small, the problem is more complicated and computationally intensive. The results here show that the stochastic system response is more sensitive to the 5th random variable compared to say the 2nd. The credible interval values suggest that they are around 15% for the dominant components. This denotes an acceptable accuracy for the evaluated sensitivity measures.

IV. Conclusions & Future Work

The corrugated skin serves as a compliant member in a flexible wing design necessary for morphing applications. Here we have studied a high fidelity model of the corrugated skin to gain a good physical insight into the effect of material and geometric uncertainties on the system response. The uncertainty analysis of a corrugated skin with random elastic parameters and uncertainty in geometric properties such as surface roughness has been analyzed to study their impact on the stochastic system response. The uncertainty propagation has been performed with the Gaussian process emulation scheme for random elastic parameters as input to the model. The statistics of the response have been obtained over the frequency range of interest and density functions have shown a good agreement with the expensive

brute force Monte Carlo method. The geometric uncertainty of the corrugated skin has been modeled with a covariance function describing the surface roughness of the skin. This is a high dimensional stochastic problem and we have used the dimension-adaptive sparse grid stochastic collocation technique with a nested Chebyshev-Gauss-Lobatto grid to obtain the system response with significantly less computational overhead. The influence of the input uncertainty on the response statistics has been analyzed with first order Sobol indices which gives the dominant components of the random variables modeling the input uncertainty.

The Bayesian metamodeling technique has been found to produce satisfactory results for the construction of a-posteriori distribution of the stochastic quantities given an input distribution. Both the Gaussian process emulation and the stochastic collocation methods rely on the solution of the stochastic system at some random points in the input stochastic space and constructing the response statistics using these sample responses. However, it must be noted that while the collocation technique is based on an analytical approximation of the solution obtained at the quadrature points with polynomial interpolation functions, the Bayesian metamodeling technique is a statistical method to evaluate the system response using the assumption that the observed outputs are realizations of a Gaussian stochastic process.

It would be interesting to look at the following aspects of uncertainty analysis of the corrugated skins in future work in this domain

- Sensitivity analysis of the corrugated skins for the various sources of input uncertainty using Sobol's measure of sensitivity, or Sobol indices.
- Investigation into the optimization of the design of corrugated skins with inputs from the uncertainty sensitivity analysis. This can provide a quantitative estimate of the geometrical parameters to which the system is sensitive.
- Propagation of the uncertainty to the equivalent low-fidelity model (ideally a simple two dimensional plate).
- Comparison of the adaptive collocation technique with the Bayesian metamodeling technique with respect to the solution accuracy and the computational efficacy.

It has to be mentioned that it is important to have an equivalent low-fidelity model of the corrugated skin which in its final form would be parametrized and used in the conceptual design of a morphing aircraft wing. Thus, we need to parametrize the response of this stochastic corrugated skin in terms of a set of equivalent elastic parameters. The propagation of input uncertainty to these equivalent parameters is a complicated exercise and would be tackled with various uncertainty propagation methods in a computationally efficient solution scheme. The impact of geometrical uncertainties in the estimation of equivalent parameters would be an important area of study.

Acknowledgments

AK acknowledges the financial support from Swansea University through the award of the Zienkiewicz scholarship. MIF acknowledge funding from the European Research Council through Grant No. 247045 entitled "Optimisation of Multi-scale Structures with Applications to Morphing Aircraft". SA acknowledges the financial support from The Royal Society of London through the Wolfson Research Merit Award.

References

[1]Guerdal, Z. and Olmedo, R., "In-plane response of laminates with spatially varying fiber orientations. Variable stiffness concept," *AIAA Journal*, Vol. 31, No. 4, 1993, pp. 751–758.

[2]Setoodeh, S., Grdal, Z., and Watson, L. T., "Design of variable-stiffness composite layers using cellular automata," *Computer Methods in Applied Mechanics and Engineering*, Vol. 195, No. 9-12, 2006, pp. 836–851.

[3]Nik, M. A., Fayazbakhsh, K., Pasini, D., and Lessard, L., "Surrogate-based multi-objective optimization of a composite laminate with curvilinear fibers," *Composite Structures*, Vol. 94, No. 8, 2012, pp. 2306–2313.

[4]Grdal, Z., Tatting, B. F., and Wu, C. K., "Variable stiffness composite panels: Effects of stiffness variation on the in-plane and buckling response," *Composites Part A: Applied Science and Manufacturing*, Vol. 39, No. 5, 2008, pp. 911–922.

[5]Ghiasi, H., Fayazbakhsh, K., Pasini, D., and Lessard, L., "Optimum stacking sequence design of composite materials Part II: Variable stiffness design," *Composite Structures*, Vol. 93, No. 1, 12 2010, pp. 1–13.

[6]Murray, G. J. and Gandhi, F., "Auxetic honeycombs with lossy polymeric infills for high damping structural materials," *21st International Conference on Adaptive Structures and Technologies 2010, ICAST 2010*, 2010, pp. 96–105.

[7]Bubert, E. A., Woods, B. K. S., Lee, K., Kothera, C. S., and Wereley, N. M., "Design and fabrication of a passive 1D morphing aircraft skin," *Journal of Intelligent Material Systems and Structures*, Vol. 21, No. 17, 2010, pp. 1699–1717.

[8]Baier, H. and Datashvili, L., "Active and morphing aerospace structures-a synthesis between advanced materials, structures and mechanisms," *International Journal of Aeronautical and Space Sciences*, Vol. 12, No. 3, 2011, pp. 225–240.

[9]Gibson, R. F., "A review of recent research on mechanics of multifunctional composite materials and structures," *Composite Structures*, Vol. 92, No. 12, 2010, pp. 2793–2810.

[10]Olympio, K. R. and Gandhi, F., "Flexible skins for morphing aircraft using cellular honeycomb cores," *Journal of Intelligent Material Systems and Structures*, Vol. 21, No. 17, 2010, pp. 1719–1735.
[11]Dietsch, B. and Tong, T., "A review - Features and benefits of shape memory polymers (SMPs)," *Journal of Advanced Materials*, Vol. 39, No. 2, 2007, pp. 3–12.
[12]Barbarino, S., Ameduri, S., Lecce, L., and Concilio, A., "Wing shape control through an SMA-based device," *Journal of Intelligent Material Systems and Structures*, Vol. 20, No. 3, 2009, pp. 283–296.
[13]Cho, M. and Kim, S., "Structural morphing using two-way shape memory effect of SMA," *International Journal of Solids and Structures*, Vol. 42, No. 5-6, 2005, pp. 1759–1776.
[14]Sofla, A. Y. N., Meguid, S. A., Tan, K. T., and Yeo, W. K., "Shape morphing of aircraft wing: Status and challenges," *Materials and Design*, Vol. 31, No. 3, 2010, pp. 1284–1292.
[15]Manzo, J., Garcia, E., Wickenheiser, A., and Horner, G. C., "Design of a shape-memory alloy actuated macro-scale morphing aircraft mechanism," Vol. 5764, Affiliation: Laboratory for Intelligent Machine Systems, 226 Upson Hall, Cornell University, Ithaca, NY 14853, United States; Affiliation: Structural Dynamics Branch, NASA Langley, Mail Stop 230, Hampton, VA 23681, United States, 2005, pp. 232–240.
[16]Calkins, F. T., Mabe, J. H., and Butler, G. W., "Boeing's variable geometry chevron: Morphing aerospace structures for jet noise reduction," Vol. 6171, Affiliation: Boeing Company, PO Box 3707, Seattle, WA 98124, United States, 2006.
[17]Georges, T., Brailovski, V., Morellon, E., Coutu, D., and Terriault, P., "Design of shape memory alloy actuators for morphing laminar wing with flexible extrados," *Journal of Mechanical Design, Transactions Of the ASME*, Vol. 131, No. 9, 2009, pp. 0910061–0910069.
[18]Yin, W., Sun, Q., Zhang, B., Liu, J., and Leng, J., *Seamless morphing wing with SMP skin*, Vol. 47-50 PART 1, 2008.
[19]Gardonio, P., "Review of active techniques for aerospace vibro-acoustic control," *Journal of Aircraft*, Vol. 39, No. 2, 2002, pp. 206–214.
[20]Kundu, A. and Berry, A., "Active sound control with smart foams using piezoelectric sensoriactuator," *Journal of Intelligent Material Systems and Structures*, Vol. 22, No. 16, 2011, pp. 1771–1787.
[21]Jr., B. F. S. and Nagarajaiah, S., "State of the art of structural control," *Journal of Structural Engineering*, Vol. 129, No. 7, 2003, pp. 845–856.
[22]Ji, H., Qiu, J., and Zhu, K., "Vibration control of a composite beam using self-sensing semi-active approach," *Chinese Journal of Mechanical Engineering (English Edition)*, Vol. 23, No. 5, 2010, pp. 663–670.
[23]Vos, R., Breuker, R. D., Barrett, R., and Tiso, P., "Morphing wing flight control via postbuckled precompressed piezoelectric actuators," *Journal of Aircraft*, Vol. 44, No. 4, 2007, pp. 1060–1068.
[24]Portela, P., Camanho, P., Weaver, P., and Bond, I., "Analysis of morphing, multi stable structures actuated by piezoelectric patches," *Computers & Structures*, Vol. 86, No. 35, 2 2008, pp. 347–356.
[25]Tawfik, S. A., Dancila, D. S., and Armanios, E., "Unsymmetric composite laminates morphing via piezoelectric actuators," *Composites Part A: Applied Science and Manufacturing*, Vol. 42, No. 7, 7 2011, pp. 748–756.
[26]Bowen, C. R., Butler, R., Jervis, R., Kim, H. A., and Salo, A. I. T., "Morphing and shape control using unsymmetrical composites," *Journal of Intelligent Material Systems and Structures*, Vol. 18, No. 1, 2007, pp. 89–98.
[27]Barbarino, S., Bilgen, O., Ajaj, R. M., Friswell, M. I., and Inman, D. J., "A review of morphing aircraft," *Journal of Intelligent Material Systems and Structures*, Vol. 22, No. 9, 2011, pp. 823–877.
[28]Thill, C., Etches, J., Bond, I., Potter, K., and Weaver, P., "Morphing skins," *Aeronautical Journal*, Vol. 112, No. 1129, 2008, pp. 117–139.
[29]Gentilini, C., Nobile, L., and Seffen, K. A., "Numerical analysis of morphing corrugated plates," Vol. 1, Affiliation: DISTART Department, University of Bologna, Viale del Risorgimento 2, Bologna 40136, Italy; Affiliation: Department of Engineering, University of Cambridge, Trumpington Street, Cambridge CB2 1PZ, United Kingdom, 2009, pp. 79–82.
[30]Ghabezi, P. and Golzar, M., "Mechanical Analysis of Trapezoidal Corrugated Composite Skins," *Applied Composite Materials*, 2012, pp. 1–13.
[31]Norman, A. D., Seffen, K. A., and Guest, S. D., "Morphing of curved corrugated shells," *International Journal of Solids and Structures*, Vol. 46, No. 7-8, 2009, pp. 1624–1633.
[32]Ge, R., Wang, B., Mou, C., and Zhou, Y., "Deformation characteristics of corrugated composites for morphing wings," *Frontiers of Mechanical Engineering in China*, Vol. 5, No. 1, 2010, pp. 73–78.
[33]Thill, C., Downsborough, J. D., Lai, S. J., Bond, I. P., and Jones, D. P., "Aerodynamic study of corrugated skins for morphing wing applications," *Aeronautical Journal*, Vol. 114, No. 1154, 2010, pp. 237–244.
[34]Yokozeki, T., i Takeda, S., Ogasawara, T., and Ishikawa, T., "Mechanical properties of corrugated composites for candidate materials of flexible wing structures," *Composites Part A: Applied Science and Manufacturing*, Vol. 37, No. 10, 2006, pp. 1578–1586.
[35]Papadrakakis, M. and Papadopoulos, V., "Robust and efficient methods for stochastic finite element analysis using Monte Carlo simulation," *Computer Methods in Applied Mechanics and Engineering*, Vol. 134, No. 3-4, 1996, pp. 325–340.
[36]Pradlwarter, H. J. and Schuller, G. I., "On advanced Monte Carlo simulation procedures in stochastic structural dynamics," *International Journal of Non-Linear Mechanics*, Vol. 32, No. 4, 1997, pp. 735 – 744, Third International Stochastic Structural Dynamics Conference.
[37]Kleiber, M. and Hien, T. D., *The Stochastic Finite Element Method*, John Wiley, Chichester, 1992.
[38]Zhu, W. Q., Ren, Y. J., and Wu, W. Q., "Stochastic FEM Based on Local Averages of Random Vector Fields," *Journal of Engineering Mechanics*, Vol. 118, No. 3, 1992, pp. 496–511.
[39]Ghanem, R. and Spanos, P. D., *Stochastic Finite Elements: A Spectral Approach*, Springer-Verlag, New York, USA, 1991.
[40]Nobile, F., Tempone, R., and Webster, C. G., "A sparse grid stochastic collocation method for partial differential equations with random input data," *SIAM Journal on Numerical Analysis*, Vol. 46, No. 5, 2008, pp. 2309–2345.
[41]Babuka, I., Nobile, F., and Tempone, R., "A stochastic collocation method for elliptic partial differential equations with random input data," *SIAM Review*, Vol. 52, No. 2, 2010, pp. 317–355.
[42]Ma, X. and Zabaras, N., "An adaptive high-dimensional stochastic model representation technique for the solution of stochastic partial differential equations," *Journal of Computational Physics*, Vol. 229, No. 10, 2010, pp. 3884–3915.
[43]Jakeman, J. D. and Roberts, S. G., *Local and dimension adaptive stochastic collocation for uncertainty quantification*, Vol. 88, 2013.
[44]O'Hagan, A., "Bayesian analysis of computer code outputs: a tutorial," *Reliability Engineering & System Safety*, Vol. 91, No. 10-11, 2006, pp. 1290–1300.
[45]Sacks, J., Welch, W., Mitchell, T., and Wynn, H., "Design and Analysis of Computer Experiments," *Statistical Science*, Vol. 4, No. 4, 1989, pp. 409–435.
[46]Santner, T., Williams, B., and Notz, W., *The Design and Analysis of Computer Experiments*, Springer Series in Statistics, London, UK, 2003.
[47]DiazDelaO, F. A. and Adhikari, S., "Structural dynamic analysis using Gaussian process emulators," *Engineering Computations*, Vol. 27, No. 5, 2010, pp. 580 – 605.
[48]E.I. Saavedra Flores, F.A. DiazDelaO, M.I. Friswell, and J. Sienz, "A computational multi-scale approach for the stochastic mechanical response of foam-filled honeycomb cores," *Composite Structures*, Vol. 94, No. 5, 2012, pp. 1861 – 1870.
[49]DiazDelaO, F. A. and Adhikari, S., "Gaussian process emulators for the stochastic finite element method," *International Journal for Numerical Methods in Engineering*, Vol. 87, No. 6, 2011, pp. 521–540.

[50]DiazDelaO, F. A. and Adhikari, S., "Bayesian assimilation of multi-fidelity finite element models," *Computers & Structures*, Vol. 92-93, No. 0, 2012, pp. 206 – 215.
[51]Saltelli, A., Annoni, P., Azzini, I., Campolongo, F., Ratto, M., and Tarantola, S., "Variance based sensitivity analysis of model output. Design and estimator for the total sensitivity index," *Computer Physics Communications*, Vol. 181, No. 2, 2010, pp. 259 – 270.
[52]Dayyani, I., Ziaei-Rad, S., and Salehi, H., "Numerical and Experimental Investigations on Mechanical Behavior of Composite Corrugated Core," *Applied Composite Materials*, Vol. 19, 2012, pp. 705–721.
[53]Xiu, D. B. and Karniadakis, G. E., "The Wiener-Askey polynomial chaos for stochastic differential equations," *Siam Journal on Scientific Computing*, Vol. 24, No. 2, 2002, pp. 619–644.
[54]Wan, X. L. and Karniadakis, G. E., "Beyond wiener-askey expansions: Handling arbitrary pdfs," *Journal of Scientific Computing*, Vol. 27, No. (-3, 2006, pp. 455–464.
[55]Matthies, H. G. and Keese, A., "Galerkin methods for linear and nonlinear elliptic stochastic partial differential equations," *Computer Methods in Applied Mechanics and Engineering*, Vol. 194, No. 12-16, 2005, pp. 1295–1331.
[56]Barthelmann, V., Novak, E., and Ritter, K., "High dimensional polynomial interpolation on sparse grids," *Advances in Computational Mathematics*, Vol. 12, No. 4, 2000, pp. 273–288.